Fluctuation-driven self-trapping in Bose-Bose mixtures

Zheng-Yan Liu, An-Chun Ji,* and Qing Sun†
Department of Physics, Capital Normal University, Beijing 100048, China

(Received 29 June 2023; accepted 23 November 2023; published 4 January 2024)

We investigate the collective dynamics of two-component Bose-Einstein condensates in a double well potential. By taking into account the Lee-Huang-Yang (LHY) correction from quantum fluctuation, we find that the LHY term, though much smaller than the mean field interactions, can significantly change the coherent oscillating behaviors of the bosonic Josephson junction in the regime of $g_{12} \simeq -\sqrt{g_{11}g_{22}}$. Besides the quantitative renormalization to the plasma frequencies of the Josephson oscillations, a series of unexpected nonzero fixed points beyond mean field emerges in the stationary state. More remarkably, unique macroscopic self-trapping states, which are usually absent in the mean field dynamics, can be sustained by the LHY nonlinearity. Our results reveal the nontrivial LHY effect on the Josephson dynamics, which can be tested in the current experiment.

DOI: 10.1103/PhysRevResearch.6.013014

I. INTRODUCTION

Quantum fluctuations around the ground state can have profound effects in the underlying systems beyond mean field. One salient example is the Lee-Huang-Yang (LHY) correction on the ground state energy of a dilute Bose gas [1,2], which may stabilize a quantum droplet state against the mean-field collapse in Bose-Bose mixtures [3–8] or dipolar gases [9–12]. More recently, by fully suppressing the mean field energy, a LHY fluid governed by quantum fluctuations was proposed [13] and observed [14]. These beyond-mean-field states highlight the importance of the LHY correction and stimulate on-going works to study the nontrivial LHY-related physics [15–23] (for reviews, see [24,25]).

In the low-energy limit, the LHY correction to the ground state energy, for a two-component Bose gas of equal mass m, takes the form of [2,3,13]

$$\mathcal{E}_{\rm LHY} = \int d\mathbf{r}\left[\frac{32\sqrt{2\pi}}{15}\frac{\hbar^2}{m}\sum_{\pm}(a_{11}n_1 + a_{22}n_2 \pm \kappa)^{\frac{5}{2}}\right], \quad (1)$$

where $\kappa = \sqrt{(a_{11}n_1 - a_{22}n_2)^2 + 4a_{12}^2 n_1 n_2}$ with n_i and a_{ij} denoting the density and scattering length, respectively. Such a contribution emerging as a nonlinear term in the Gross-Pitaevskii (GP) description [3,24] would change the dynamics of the condensate. Of particular interest, if a double-well-like potential is applied to achieve a Bose-Josephson junction (BJJ) [26], a natural question arises: how are the bosonic Josephson physics [27–32], such as the notable macroscopic quantum self-trapping (MQST) [33,34], as well as the Josephson oscillations being affected by the LHY term? Specifically, in the regime of a competing interspecies attraction [3,13] where the mean-field energy is suppressed, the intriguing LHY effects may become prominent, which however has never been revealed so far.

In this work, we study the collective dynamics of a binary Bose-Einstein condensate (BECs) in a double well potential [35–40]. By taking into account the quantum LHY correction, we find that the nonlinear LHY term, though much smaller than the mean field interactions, can significantly change the coherent oscillations of the condensates, giving rise to rich dynamical behaviors with unique features. It shows that the LHY term can considerably renormalize the frequencies of the plasma oscillations in the Josephson regime. More remarkably, the LHY term itself can drive a dynamical transition to distinct MQST phases, in sharp contrast to the mean-field correspondence where such MQST is usually absent. We attribute this to the LHY nonlinearity induced nontrivial fixed points of the underlying dynamical equations beyond mean field. These results, which are accessible in the current experiment, reveal the nontrivial role played by the quantum fluctuation in the bosonic Josephson effects and open an avenue to investigate the intriguing LHY physics beyond mean field in a dynamical way.

II. MODEL AND FORMULISM

We consider a binary BECs comprised of two internal states (labeled as $i = 1, 2$) confined in a symmetric double-well potential. In the presence of the LHY correction given by Eq. (A2), the dynamics of the condensates can be described by the modified Gross-Pitaevskii equations [24]

$$i\hbar\frac{\partial \Psi_i}{\partial t} = \left[-\frac{\hbar^2}{2m}\nabla^2 + V_{\rm dw} + \sum_j g_{ij}n_j + \frac{128\sqrt{\pi}}{3}\frac{\hbar^2}{m}a_{ii}(a_{11}n_1 + a_{22}n_2)^{\frac{3}{2}}\right]\Psi_i, \quad (2)$$

*andrewjee@sina.com
†sunqing@cnu.edu.cn

where $\Psi_i(\mathbf{r})$ is the condensate wave function for the ith component $n_i = |\Psi_i|^2$, and $g_{ij} = 4\pi\hbar^2 a_{ij}/m$ is the interaction strength between component i and j. $V_{\rm dw}$ is a symmetric state-independent double-well like potential [41]. For simplicity, here we have assumed a competing (attractive) interaction $g_{12} = -\sqrt{g_{11}g_{22}}$ $(g_{11}, g_{22} > 0)$ such that the lower branch in $\mathcal{E}_{\rm LHY}$ is vanishing.

Within the two-mode approximation for each component, we can expand $\Psi_i \simeq \psi_{iL}(t)\Phi_L(\mathbf{r}) + \psi_{iR}(t)\Phi_R(\mathbf{r})$ with the ground state $\Phi_{L(R)}(\mathbf{r})$ of the isolated left (right) well, and derive the coupled motional equations for the amplitudes $\psi_{iL(R)} \equiv \sqrt{N_{iL(R)}}e^{i\theta_{iL(R)}}$ with $N_{iL(R)}$ and $\theta_{iL(R)}$ being the atom number and phase of the ith component in the left (right) well, which are given by

$$i\hbar\frac{\partial\psi_{iL}}{\partial t} = \left[E_i^L + \sum_j U_{ij}^L N_{jL} + \alpha_{\rm LHY}^L a_{ii}(a_{11}N_{1L} + a_{22}N_{2L})^{\frac{3}{2}}\right]\psi_{iL} - J\psi_{iR}, \tag{3a}$$

$$i\hbar\frac{\partial\psi_{iR}}{\partial t} = \left[E_i^R + \sum_j U_{ij}^R N_{jR} + \alpha_{\rm LHY}^R a_{ii}(a_{11}N_{1R} + a_{22}N_{2R})^{\frac{3}{2}}\right]\psi_{iR} - J\psi_{iL}. \tag{3b}$$

Here, $E_i^{L(R)}$, $U_{ij}^{L(R)}$, J, and $\alpha_{\rm LHY}^{L(R)}$ are parameters characterizing the intrawell energy, atom-atom interactions, interwell tunneling, and LHY correction, respectively. For a symmetric potential, we have $E_i^L = E_i^R$, $U_{ij}^L = U_{ij}^R \equiv U_{ij}$, and $\alpha_{\rm LHY}^L = \alpha_{\rm LHY}^R \equiv \alpha_{\rm LHY}$.

In terms of the relative particle number difference $z_i = \frac{N_{iL}-N_{iR}}{N_i}$ and phase difference $\phi_i = \theta_{iR} - \theta_{iL}$, Eq. (3) can be recast as ($\hbar = 1$),

$$\dot{z}_i = -\sqrt{1-z_i^2}\sin\phi_i, \tag{4a}$$

$$\dot{\phi}_i = \Lambda_{\rm MF}(-\gamma)^{(i-1)}(z_1 - \gamma z_2) + \frac{z_i}{\sqrt{1-z_i^2}}\cos\phi_i + \Lambda_{\rm LHY}\gamma^{2(i-1)}f_\gamma(z_1, z_2), \tag{4b}$$

with

$$f_\gamma = (z_1 + \gamma^2 z_2)\frac{1+\gamma^2+\frac{1}{2}\sqrt{(1+\gamma^2)^2-(z_1+\gamma^2 z_2)^2}}{\sqrt{1+\gamma^2+\sqrt{(1+\gamma^2)^2-(z_1+\gamma^2 z_2)^2}}}.$$

Here we have rescaled the time as $2Jt \to t$ and introduced dimensionless parameters $\Lambda_{\rm MF} = U_{11}N/4J$, $\Lambda_{\rm LHY} = \alpha_{\rm LHY}a_{11}^{\frac{5}{2}}(\frac{N}{2})^{\frac{3}{2}}/2J$, and $\gamma^2 = U_{22}/U_{11} \geqslant 1$. $N = N_1 + N_2$ is the total atom number, and in this work we consider an equal population of both components, i.e., $N_1 = N_2 = N/2$. Despite the complicated form of LHY correction to the (relative) phase variation, it respects a Z_2 symmetry, i.e., Eq. (4) is invariant under the transformation $z_i \to -z_i$ and $\phi_i \to -\phi_i$.

In a semiclassic correspondence, Eq. (4) describes the dynamics of two coupled nonrigid pendulums, where the conjugate variables $\{z_i, \phi_i\}$ obeying the canonical relations $\dot{z}_i = -\frac{\partial H}{\partial\phi_i}$ and $\dot{\phi}_i = \frac{\partial H}{\partial z_i}$ are governed by the Hamiltonian

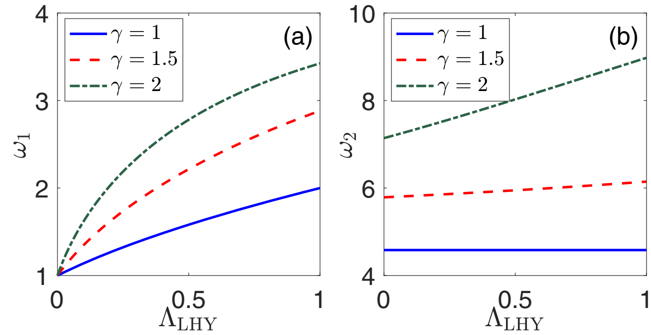

FIG. 1. Plasma frequencies ω_1 (a) and ω_2 (b) as functions of $\Lambda_{\rm LHY}$ for different $\gamma = 1$ (blue solid), 1.5 (red dashed), and 2 (green dash dotted). Here, $\Lambda_{\rm MF} = 10$.

$$H = \frac{\Lambda_{\rm MF}}{2}(z_1-\gamma z_2)^2 - \sum_i\sqrt{1-z_i^2}\cos\phi_i + \Lambda_{\rm LHY}[(1+\gamma^2)^2 \times (1+\gamma^2+\sqrt{(1+\gamma^2)^2-(z_1+\gamma^2 z_2)^2})^{\frac{1}{2}} - \frac{1}{5}(1+\gamma^2+\sqrt{(1+\gamma^2)^2-(z_1+\gamma^2 z_2)^2})^{\frac{5}{2}}]. \tag{5}$$

It's interesting to see that the LHY term introduces a fractional power nonlinearity on the "angular momentum" z_i, which dictates the dynamical behaviors of two-component BJJ in the LHY regime $\Lambda_{\rm LHY}/\mathcal{J} \sim 1$, and leads to rich physics beyond mean field.

III. JOSEPHSON OSCILLATIONS

For small amplitude oscillations ($|z_i|, |\phi_i| \ll 1$) around the ground state $z_{i,0} = \phi_{i,0} = 0$, Eq. (4) can be linearized as

$$\dot{z}_i \simeq -\phi_i, \tag{6a}$$

$$\dot{\phi}_i \simeq \Lambda_{\rm MF}(-\gamma)^{(i-1)}(z_1 - \gamma z_2) + \Lambda_{\rm LHY}\gamma^{2(i-1)}\tilde{f}_\gamma(z_1+\gamma^2 z_2) + z_i, \tag{6b}$$

where $\tilde{f}_\gamma = \frac{3}{2}\sqrt{\frac{1+\gamma^2}{2}}$. Solving the above equations we can obtain two eigenmodes of the linear sinusoidal oscillations with the Josephson plasma frequencies $\omega_{1,2}$, as shown in Figs. 1(a) and 1(b). For a symmetric interaction $\gamma = 1$, these two modes reduce to $z_1(t) = z_2(t) \sim \sin(\omega_1 t)$ with $\omega_1 = \sqrt{3\Lambda_{\rm LHY}+1}$, and $z_1(t) = -z_2(t) \sim \sin(\omega_2 t)$ with $\omega_2 = \sqrt{2\Lambda_{\rm MF}+1}$, in analog to the in-phase and out-of-phase librations of two coupled pendulums. As $\Lambda_{\rm MF} \gg \Lambda_{\rm LHY}$, one has $\omega_2 \gg \omega_1$ corresponding to the collective (slow) density and (fast) spin oscillations, respectively. Note that, though the LHY term does not affect the spin oscillation (ω_2), it remarkably renormalizes the oscillating frequency ω_1 of the density, in contrast to the mean-field $\omega_{1,\rm MF} = 2\mathcal{J}$ where the LHY correction is absent. For asymmetric interactions $\gamma > 1$, the decoupled density and spin modes at $\gamma = 1$ get mixed, with both frequencies $\omega_{1,2}$ being changed considerably.

Beyond the linear regime, a full simulation of Eq. (4) gives generalized nonsinusoidal Josephson oscillations of z_i and ϕ_i due to the intrinsic anharmonicity. Specifically, when the

TABLE I. Nonzero fixed points and their stabilities ($\gamma = 1$).

ϕ_1^s/ϕ_2^s	$\pm(z_1^s/z_2^s)\,(\Lambda_{\rm LHY} = 0)$	$\pm(z_1^s/z_2^s)\,(\Lambda_{\rm LHY} > 0)$
π/π	$z_1^s = -z_2^s > 0$ ($\Lambda_{\rm MF} > \frac{1}{2}$), stable.	(i) $z_1^s = -z_2^s > 0$ ($\Lambda_{\rm MF} > \frac{1}{2}$), stable; (ii) $z_1^s = z_2^s > 0$ ($\Lambda_{\rm LHY} > \frac{1}{3}$), stable ($\Lambda_{\rm LHY} \geqslant \Lambda_{\rm LHY}^*$); (iii) $z_1^s > z_2^s > 0, z_2^s > z_1^s > 0$ ($\Lambda_{\rm LHY} > \Lambda_{\rm LHY}^*$), unstable.
$\pi/0$	None[a]	$z_1^s > z_2^s > 0$ ($\Lambda_{\rm LHY} > \frac{1}{6\Lambda_{\rm MF}}$); stable.
$0/\pi$	None	$z_2^s > z_1^s > 0$ ($\Lambda_{\rm LHY} > \frac{1}{6\Lambda_{\rm MF}}$), stable [42].
$0/0$	None	None

[a]"None" means that the nonzero fixed point does not exist.

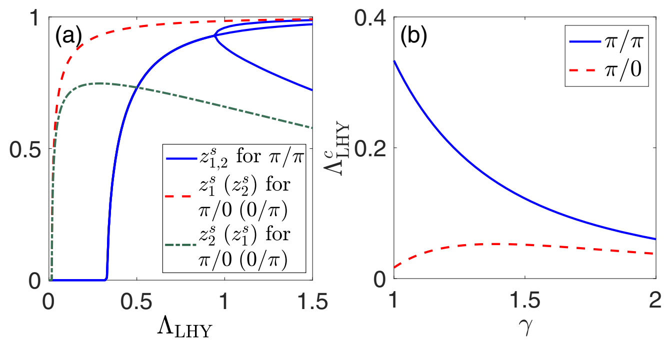

FIG. 2. (a) Evolution of the nonzero fixed points versus $\Lambda_{\rm LHY}$ for $\phi_1^s/\phi_2^s = \pi/\pi$ (blue solid) and $\pi/0$, $0/\pi$ (red dashed and green dash dotted) at $\gamma = 1$; (b) Critical $\Lambda_{\rm LHY}^c$ versus γ for $\phi_1^s/\phi_2^s = \pi/\pi$ (blue solid) and $\pi/0$ (red dashed). $\Lambda_{\rm MF} = 10$.

nonlinear interactions are dominant, a remarkable phenomenon known as the MQST [33] may appear in the BJJ, where the Z_2 symmetry is dynamically broken with a spontaneous population imbalance of atoms in the double well. As we will show in below that the LHY term, though much smaller than the strength of the mean-field interactions, can lead to unique MQST states beyond mean field.

IV. FIXED POINT AND STABILITY ANALYSIS

We proceed by considering the fixed points of Eqs. (4), which characterize the possible MQST around a stationary state. By setting all the derivatives as zero in Eq. (4), we have $\phi_i^s = 0$ or π while z_i^s is generally obtained by numerically solving two coupled equations [41]. Then for small perturbations around the fixed point, i.e., $(z_i, \phi_i) = (z_i^s + \delta z_i, \phi_i^s + \delta\phi_i)$, we linearize Eq. (4) to obtain $(\ddot{\delta z_1}, \ddot{\delta z_2})^T = \mathcal{M}(\delta z_1, \delta z_2)^T$ with $\mathcal{M}$ being the drift matrix and $(\cdots)^T$ denoting the transposition. Diagonalizing $\mathcal{M}$ to obtain two eigenfrequencies $-\omega_\pm^2$, a stable fixed point requires $\omega_\pm^2 \geqslant 0$. There always exists a zero solution $z_1^s = z_2^s = 0$, while the nonzero fixed points and their stabilities for different cases at $\gamma = 1$ are listed in Table I, where $\pm$ reflects the Z_2 symmetry. One can see that in the presence of a LHY term, a series of new fixed points beyond mean field arise.

For $\gamma = 1$, a symmetric solution $z_1^s = z_2^s \neq 0$ develops at a critical $\Lambda_{\rm LHY}^c = 1/3$ for the case $\phi_1^s/\phi_2^s = \pi/\pi$, which increases quickly with $\Lambda_{\rm LHY}$, as shown in Fig. 2(a). Such a symmetric fixed point emerging from the spin-exchanging symmetry becomes stable when $\Lambda_{\rm LHY} \geqslant \Lambda_{\rm LHY}^*$ with

$$\Lambda_{\rm LHY}^* = \frac{(2\Lambda_{\rm MF})^{1/3}\sqrt{1 + 1/(2\Lambda_{\rm MF})^{1/3}}}{\sqrt{2}(2 + 1/(2\Lambda_{\rm MF})^{1/3})},$$

across which another two unstable asymmetric solutions set up. While for the case $\phi_1^s/\phi_2^s = \pi/0$ ($0/\pi$), an asymmetric $z_1^s > z_2^s > 0$ ($z_2^s > z_1^s > 0$) can be found for $\Lambda_{\rm LHY} > \Lambda_{\rm LHY}^c = 1/6\Lambda_{\rm MF}$. These nontrivial fixed points (for most of the cases) are dynamically stable and can only exist in the presence of LHY correction, in contrast to the soly antisymmetric solution $z_1^s = -z_2^s = \pm\sqrt{1 - 1/4\Lambda_{\rm MF}^2}$ ($\Lambda_{\rm MF} > 1/2$) of the π/π case in the mean field.

For $\gamma > 1$, due to the breaking of Z_2-type spin-exchanging symmetry, the nonzero solutions are generally asymmetric with the critical $\Lambda_{\rm LHY}^c$ shown in Fig. 2(b). For the π/π case, $\Lambda_{\rm LHY}^c$ decreases with γ and approaches $\frac{2\sqrt{2}\sqrt{\gamma^2+1}}{3\gamma^2(\gamma+1)^2}$ for $\Lambda_{\rm MF} \gg 1$. While for the $\pi/0$ case, $\Lambda_{\rm LHY}^c \to \frac{2\sqrt{2}(\gamma-1)}{3\sqrt{\gamma^2+1}\gamma^2(\gamma+1)}$ depends nonmonotonically on γ. Note that for the $0/\pi$ case (refer to Table II), we have $\Lambda_{\rm LHY}^c = 0$ for $\gamma = \sqrt{1 + 1/\Lambda_{\rm MF}}$, meaning that the LHY-induced nonzero solution in this case can survive in the mean field for sufficient asymmetric interactions. We have also examined the stabilities of these nonzero fixed points and find that most of them are stable, as summarized in Table II.

The emerging of the nontrivial fixed points brought by the LHY correction can not only manifest as self-trapping of the atomic populations in steady states, but also indicate that more interested dynamical MQST with $\langle z_i(t)\rangle \neq 0$ beyond mean field may appear in this system when away from the fixed points.

V. FLUCTUATION-DRIVEN SELF-TRAPPING

Generally speaking, the dynamical MQST happens when the nonlinear interaction energy of an initial state is dominant over the kinetic energy (tunneling). To distill the effect of LHY term, we are interested in the regime of $z_1(0) \sim \gamma z_2(0)$ where the initial mean-field interaction energy of the state is nearly vanishing. In this case, the MQST is always absent for arbitrary initial phase $\phi_i(0)$ and mean-field interaction $\Lambda_{\rm MF} > 0$ if $\Lambda_{\rm LHY} = 0$. The including of the LHY correction can significantly change the mean-field scenario, and we will see below that a finite but small $\Lambda_{\rm LHY}$ would sustain a high-lying self-trapping state due to the positive energy corrections from quantum fluctuations. For simplicity, we first assume $\phi_1(0) = \phi_2(0)$. For $\gamma = 1$, both components exhibit the same evolution behaviors governed by

$$\dot{z} = -\sqrt{1 - z^2}\sin\phi, \qquad (7a)$$

$$\dot{\phi} = \frac{z}{\sqrt{1 - z^2}}\cos\phi + \sqrt{2}\Lambda_{\rm LHY} z \frac{2 + \sqrt{1 - z^2}}{\sqrt{1 + \sqrt{1 - z^2}}}, \qquad (7b)$$

TABLE II. Nonzero fixed points and their stabilities for $\gamma > 1$.

ϕ_1^s/ϕ_2^s	$\pm(z_1^s, z_2^s)$ $(\Lambda_{LHY} = 0)$	$\pm(z_1^s, z_2^s)$ $(\Lambda_{LHY} > 0)$
π/π	$z_1^s > -z_2^s > 0$ for $\Lambda_{MF} > \frac{1}{1+\gamma^2}$, stable.	$z_1^s > -z_2^s > 0$ for $\Lambda_{MF} > \frac{1}{1+\gamma^2}$, stable; $z_1^s > z_2^s > 0$ for $\Lambda_{LHY} > \frac{2\sqrt{2}}{3\sqrt{1+\gamma^2}} \frac{\Lambda_{MF}+\Lambda_{MF}\gamma^2-1}{\Lambda_{MF}\gamma^2+2\Lambda_{MF}\gamma^3+\Lambda_{MF}\gamma^4-\gamma^4-1}$, unstable.
$\pi/0$	None.	$z_1^s > z_2^s > 0$ for $\Lambda_{LHY} > \frac{2\sqrt{2}}{3\sqrt{1+\gamma^2}} \frac{-\Lambda_{MF}+\Lambda_{MF}\gamma^2+1}{\Lambda_{MF}\gamma^2+2\Lambda_{MF}\gamma^3+\Lambda_{MF}\gamma^4-\gamma^4+1}$, stable for $\Lambda_{LHY} \leqslant \Lambda_{LHY}^{\star,1}$ or $\Lambda_{LHY} \geqslant \Lambda_{LHY}^{\star,2}$ [a].
$0/\pi$	$z_2^s > z_1^s > 0$ for $\Lambda_{MF} > \frac{1}{\gamma^2-1}$, stable.	$z_2^s > z_1^s > 0$ for $\Lambda_{MF} > \frac{1}{\gamma^2-1}$, stable; $z_2^s > z_1^s > 0$ for $\Lambda_{LHY} > \frac{2\sqrt{2}}{3\sqrt{1+\gamma^2}} \frac{\Lambda_{MF}-\Lambda_{MF}\gamma^2+1}{\Lambda_{MF}\gamma^2+2\Lambda_{MF}\gamma^3+\Lambda_{MF}\gamma^4+\gamma^4-1}$ and $\Lambda_{MF} < \frac{1}{\gamma^2-1}$, stable.
$0/0$	None.	None.

[a] The imaginary parts of the eigenfrequencies $\omega_\pm$ are nonzero for $\Lambda_{LHY}^{\star,1} < \Lambda_{LHY} < \Lambda_{LHY}^{\star,2}$, see [41] for more details.

where $z_1 = z_2 \equiv z$ and $\phi_1 = \phi_2 \equiv \phi$. Compared to the mean-field dynamics of a single-component BJJ [33], here the atomic nonlinearity fully depends on the LHY correction.

From Eq. (7), a dynamical MQST of z emerges when the energy of an initial state is larger than the threshold $E_{th} = 2 + \frac{8}{5}\Lambda_{LHY}$. This can be achieved if $\Lambda_{LHY} > \Lambda_{LHY}^{th}$ with

$$\Lambda_{LHY}^{th} = \frac{1 + \sqrt{1 - z^2(0)}\cos\phi(0)}{2\sqrt{2}[(1+\sqrt{1-z^2(0)})^{\frac{1}{2}} - \frac{1}{5}(1 + \sqrt{1 - z^2(0)})^{\frac{5}{2}}] - \frac{4}{5}}. \tag{8}$$

In Figs. 3(a) and 3(b), we show the dynamical evolution of $z(t)$ and the corresponding energy contour given by Eq. (5) in the z-ϕ space under the initial conditions $z(0) = 0.6$ and $\phi(0) = \pi$ for different Λ_{LHY}. With the increasing of Λ_{LHY}, a dynamical transition from sinusoid-type oscillations around $z = 0$ to anharmonic oscillation with nonzero $\langle z(t)\rangle \neq 0$ can be clearly identified, suggesting the MQST arises for $\Lambda_{LHY} > \Lambda_{LHY}^{th} \simeq 0.3733$ from Eq. (8).

Such a LHY driven self-trapping can also be found for more general γ (>1) and $\phi_1(0) \neq \phi_2(0)$. For example, in Figs. 3(c) and 3(d), we show the evolutions of $z_i(t)$ and $\phi_i(t)$ at $\gamma = 1.5$ for $\phi_1(0)/\phi_2(0) = \pi/0$. There are two types of self-trapping states: for small Λ_{LHY} in Fig. 3(c), both $z_i(t)$ and $\phi_i(t)$ exhibit small-amplitude oscillations; while for relatively large Λ_{LHY} in Fig. 3(d), $z_i(t)$ shows large-amplitude oscillation and the phase $\phi_i(t)$ begins to run, corresponding to the so-called "π phase" and "running phase" MQST [34]. Notice that the required LHY parameter to trigger the MQST for $\gamma > 1$ is much smaller than the symmetric case, facilitating the observation in realistic experiments. We would like to point out that, besides the regular oscillating behaviors discussed above, irregular oscillations with chaotic features [43–45] may be also found in this system especially in the regime of large Λ_{LHY}, which however, is beyond the scope of this work and we leave it for the future study.

VI. DISCUSSION AND CONCLUSION

So far, we have focused on a competing interaction with $\delta g \equiv 1 + g_{12}/\sqrt{g_{11}g_{22}} = 0$, which may be not exactly tuned in experiment. Deviating from $\delta g = 0$, both branches in Eq. (A2) would contribute to the dynamics in general [41]. In Fig. 4, we plot the critical Λ_{LHY}^c as a function of δg. One can see Λ_{LHY}^c decreases with δg gradually, indicating that the main results governed by the LHY term would not be changed essentially until a sufficiently large δg beyond which the mean field interactions take over.

In the experiment, the BJJ has been realized in diverse setups [27,28,32], where arbitrary initial conditions can be generally prepared and the dominating mean field dynamics is observed. To detect the LHY effect reported in this work, one

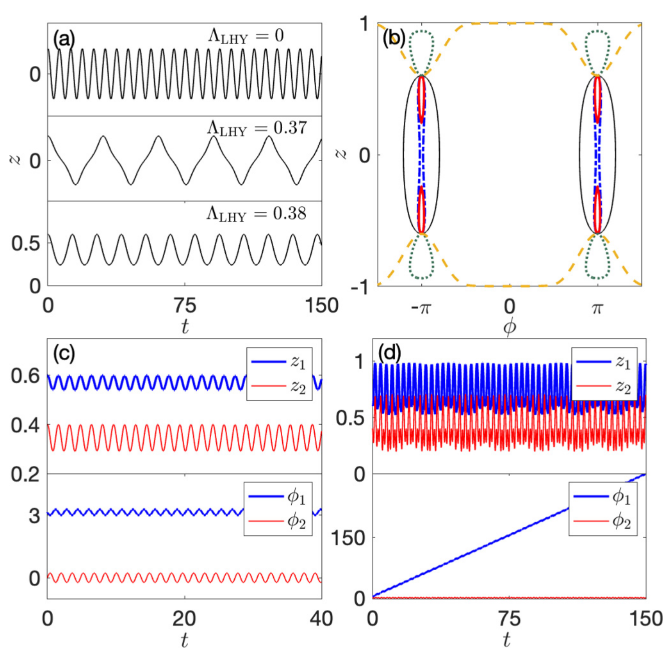

FIG. 3. (a) Time evolution of $z(t)$ for $\Lambda_{LHY} = 0$ (top), 0.37 (middle), and 0.38 (bottom); (b) Constant energy contour in the z-ϕ plane for $\Lambda_{LHY} = 0$ (black thin solid), 0.37 (blue dash dotted), 0.38 (red solid), 0.6 (yellow dashed), and 0.9 (green dotted), respectively; Time evolutions of $z_i(t)$ and $\phi_i(t)$ at $\gamma = 1.5$ for (c) $\Lambda_{LHY} = 0.07$ and (d) $\Lambda_{LHY} = 0.2$. The initial conditions are $[z(0), \phi(0)] = [0.6, \pi]$ for (a) and (b), and $[z_1(0), \phi_1(0), z_2(0), \phi_2(0)] = [0.6, \pi, 0.4, 0]$ for (c) and (d). $\Lambda_{MF} = 10$.

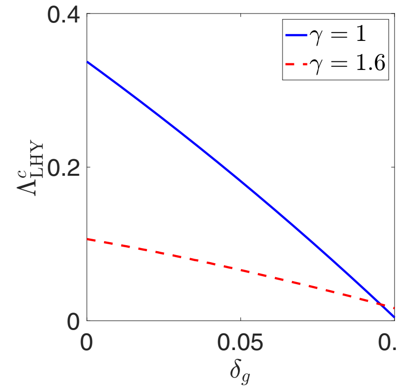

FIG. 4. Critical $\Lambda^c_{\rm LHY}$ as a function of δg for $\gamma = 1$ (blue solid) and 1.6 (red dashed). Here $\phi_1^s/\phi_2^s = \pi/\pi$ and $\Lambda_{\rm MF} = 10$.

can tune the interactions to the regime of $\delta g \approx 0$ by the Feshbach resonance [46]. For example, the competing interactions of two hyperfine states $|1, -1\rangle$ and $|1, 0\rangle$ of ^{39}K [14] are $a_{11} \simeq 33.3a_0$, $a_{22} \simeq 84.2a_0$, and $a_{12} \simeq -53.2a_0$ (a_0 the Bohr radius) with $\gamma = \sqrt{a_{22}/a_{11}} \simeq 1.6$; this gives the critical $\Lambda_{\rm LHY} \approx 0.06$ and 0.16 of the two types of MQST in Figs. 3(c) and 3(d) with the same initial conditions. Considering the LHY correction is about several percents of the mean field energy for the typical atomic density with gas parameter $na^3 \sim 10^{-5} - 10^{-4}$ [47], the LHY parameter $\Lambda_{\rm LHY}$ can be tuned by varying the mean field $\Lambda_{\rm MF}$ and/or the interwell tunneling $\mathcal{J}$ to address the relevant regime in this work.

To conclude, we have investigated the LHY effect on the collective dynamics of a two-component BJJ. A remarkable dynamical transition to unique self-trapping states together with a series of nontrivial fixed points beyond mean field are predicted to appear even for a tiny LHY correction, which arises from the quantum fluctuations. Our work paves a new way to explore the unusual LHY physics within the current experiment. Future studies may include the Josephson effect in the droplet regime with $\delta g < 0$, the LHY effect on the chaotic dynamics of the BJJ and the Measure synchronization [48,49].

ACKNOWLEDGMENTS

This work was supported by the NSFC under Grants No. 12375017 and No. 62175169.

APPENDIX A: DERIVATION OF THE MODEL

We consider a binary Bose-Einstein condensate (BECs) comprised of two internal states (labeled as $i = 1, 2$) of mass m in a double-well potential, with the mean field energy given by

$$\mathcal{E}_{\rm MF} = \int d\mathbf{r} \sum_{i=1,2} \Psi_i^*(\mathbf{r})[-\frac{\hbar^2\nabla^2}{2m} + V_{\rm dw}(\mathbf{r}) + \frac{1}{2}\sum_{j=1,2} g_{ij} n_j(\mathbf{r})]\Psi_i^*(\mathbf{r}), \quad \text{(A1)}$$

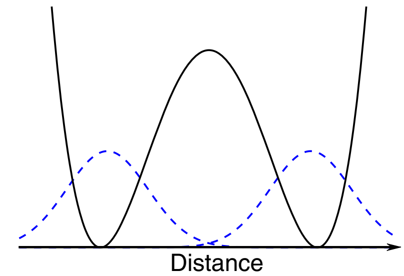

FIG. 5. Schematic of the double-well potential.

where $n_i = |\Psi_i|^2$ is the density with $\Psi_i(\mathbf{r})$ ($i = 1, 2$) being the condensate wave function for the ith component. $g_{ij} = 4\pi\hbar^2 a_{ij}/m$ represents the strength of the contact interaction between the atoms of component i and j with a_{ij} being the corresponding s-wave scattering length. $V_{\rm dw}$ is a (symmetric) state-independent double-well-like potential (see Fig. 5), which for instance may be formed by splitting a trap into two parts with a periodic potential [27] or using a single periodic unit of an optical superlattice [32]. Beyond mean field, the quantum fluctuations would contribute to the ground state energy. To the leading order, it gives to the notable LHY correction, which, for the two-component Bose gas, is

$$\mathcal{E}_{\rm LHY} = \int d\mathbf{r}\left[\frac{32\sqrt{2\pi}}{15}\frac{\hbar^2}{m}\sum_{\pm}(a_{11}n_1 + a_{22}n_2 \pm \sqrt{(a_{11}n_1 - a_{22}n_2)^2 + 4a_{12}^2 n_1 n_2})^{\frac{5}{2}}\right]. \quad \text{(A2)}$$

In this work, we are interested in the regime of competing (attractive) interactions with $g_{12} \simeq -\sqrt{g_{11}g_{22}}$ ($g_{11}, g_{22} > 0$), i.e., $a_{12} \simeq -\sqrt{a_{11}a_{22}}$ ($a_{11}, a_{22} > 0$), where the mean field interactions are (partly) suppressed. To proceed, we first consider $g_{12} = -\sqrt{g_{11}g_{22}}$, i.e., $\delta g \equiv g_{12} + \sqrt{g_{11}g_{22}} = 0$. In this case, the lower "$-$" branch in Eq. (A2) is vanishing. Then, the dynamics of the condensates in the presence of LHY correction can be described by the modified Gross-Pitaevskii equations [24]

$$i\hbar\frac{\partial\Psi_1}{\partial t} = \left[-\frac{\hbar^2\nabla^2}{2m} + V_{\rm dw} + g_{11}n_1 + g_{12}n_2 + \frac{128\sqrt{\pi}}{3}\frac{\hbar^2}{m}a_{11}(a_{11}n_1 + a_{22}n_2)^{\frac{3}{2}}\right]\Psi_1, \quad \text{(A3a)}$$

$$i\hbar\frac{\partial\Psi_2}{\partial t} = \left[-\frac{\hbar^2\nabla^2}{2m} + V_{\rm dw} + g_{12}n_1 + g_{22}n_2 + \frac{128\sqrt{\pi}}{3}\frac{\hbar^2}{m}a_{22}(a_{11}n_1 + a_{22}n_2)^{\frac{3}{2}}\right]\Psi_2. \quad \text{(A3b)}$$

For weakly interacting BECs in a double-well potential, the two-mode approximation can be applied, and we expand the condensate wave function Ψ_i as

$$\Psi_i(\mathbf{r}, t) \simeq \psi_{iL}(t)\Phi_L(\mathbf{r}) + \psi_{iR}(t)\Phi_R(\mathbf{r}), \quad \text{(A4)}$$

where $\psi_{iL(R)}(t)$ is the time-dependent amplitude and $\Phi_{L(R)}(\mathbf{r})$ is the ground state in the isolated left (right) well, satisfying

$$\int d\mathbf{r}|\Phi_L|^2 = \int d\mathbf{r}|\Phi_R|^2 = 1,$$
$$\int d\mathbf{r}\Phi_L^{*m}\Phi_R^n = \int d\mathbf{r}\Phi_R^{*n}\Phi_L^m \simeq 0\,(m,n \geqslant 1), \tag{A5}$$

$$N_i = \int d\mathbf{r}|\Psi_i|^2 = \int d\mathbf{r}|\psi_{iL}|^2 + \int d\mathbf{r}|\psi_{iR}|^2 = N_{iL} + N_{iR}. \tag{A6}$$

Substituting Eq. (A4) into Eq. (A3) and taking use of Eq. (A5), we arrive at the dynamical equations for the amplitudes $\psi_{iL(R)}$ $(i = 1, 2)$:

$$i\hbar\frac{\partial\psi_{iL}}{\partial t} = \left[E_i^L + \sum_j U_{ij}^L|\psi_{jL}|^2 + \alpha_{\mathrm{LHY}}^L a_{ii}(a_{11}|\psi_{1L}|^2 + a_{22}|\psi_{2L}|^2)^{\frac{3}{2}}\right]\psi_{iL} - J\psi_{iR}, \tag{A7a}$$

$$i\hbar\frac{\partial\psi_{iR}}{\partial t} = \left[E_i^R + \sum_j U_{ij}^R|\psi_{jR}|^2 + \alpha_{\mathrm{LHY}}^R a_{ii}(a_{11}|\psi_{1R}|^2 + a_{22}|\psi_{2R}|^2)^{\frac{3}{2}}\right]\psi_{iR} - J\psi_{iL}, \tag{A7b}$$

where

$$\begin{aligned} E_i^{L(R)} &= \int d\mathbf{r}\Phi_{L(R)}^*\left(-\frac{\hbar^2}{2m}\nabla^2 + V_{\mathrm{dw}}\right)\Phi_{L(R)}, \\ U_{ij}^{L(R)} &= g_{ij}\int d\mathbf{r}|\Phi_{L(R)}|^4, \\ \alpha_{\mathrm{LHY}}^{L(R)} &= \frac{128\sqrt{\pi}}{3}\frac{\hbar^2}{m}\int d\mathbf{r}|\Phi_{L(R)}|^5, \\ J &= -\int d\mathbf{r}\Phi_L^*\left(-\frac{\hbar^2}{2m}\nabla^2 + V_{\mathrm{dw}}\right)\Phi_R \end{aligned} \tag{A8}$$

are parameters characterizing the intrawell energy, mean-field interaction, LHY correction, and interwell tunneling, respectively. For a symmetric potential considered in this work, we have $E_i^L = E_i^R$, $U_{ij}^L = U_{ij}^R \equiv U_{ij}$, and $\alpha_{\mathrm{LHY}}^L = \alpha_{\mathrm{LHY}}^R \equiv \alpha_{\mathrm{LHY}}$.

By writing $\psi_{iL(R)} \equiv \sqrt{N_{iL(R)}}e^{i\theta_{iL(R)}}$ with $N_{iL(R)}$ and $\theta_{iL(R)}$ being the atom number and phase of the ith component in the left (right) well, and further introducing the relative particle number difference $z_i = \frac{N_{iL}-N_{iR}}{N_i}$ and phase difference $\phi_i = \theta_{iR} - \theta_{iL}$, Eq. (A7) can be rewritten as ($\hbar = 1$),

$$\begin{aligned} \dot{z}_i &= -2J\sqrt{1-z_i^2}\sin\phi_i, \\ \dot{\phi}_i &= \sum_{j=1,2} U_{ij}N_j z_j + 2J\frac{z_i}{\sqrt{1-z_i^2}}\cos\phi_i + \alpha_{\mathrm{LHY}}a_{ii}f(z_1,z_2), \end{aligned} \tag{A9}$$

where

$$f(z_1,z_2) = \frac{(a_{11}N_1z_1 + a_{22}N_2z_2)(a_{11}N_1 + a_{22}N_2 + \frac{1}{2}\sqrt{(a_{11}N_1 + a_{22}N_2)^2 - (a_{11}N_1z_1 + a_{22}N_2z_2)^2})}{\sqrt{a_{11}N_1 + a_{22}N_2 + \sqrt{(a_{11}N_1 + a_{22}N_2)^2 - (a_{11}N_1z_1 + a_{22}N_2z_2)^2}}}. \tag{A10}$$

For a balanced population of both components, i.e., $N_1 = N_2 = \frac{N}{2}$ with N the total particle number, by introducing dimensionless parameters $\Lambda_{\mathrm{MF}} = U_{11}N/4J$, $\Lambda_{\mathrm{LHY}} = \alpha_{\mathrm{LHY}}a_{11}^{\frac{5}{2}}(\frac{N}{2})^{\frac{3}{2}}/2J$, and $\gamma = \sqrt{U_{22}/U_{11}} \geqslant 1$, and rescaling the time as $2Jt \to t$, we finally obtain the dynamical equations (4a) and (4b) in the main text, which are

$$\begin{aligned} \dot{z}_i &= -\sqrt{1-z_i^2}\sin\phi_i, \\ \dot{\phi}_i &= \Lambda_{\mathrm{MF}}(-\gamma)^{(i-1)}(z_1 - \gamma z_2) + \frac{z_i}{\sqrt{1-z_i^2}}\cos\phi_i + \Lambda_{\mathrm{LHY}}\gamma^{2(i-1)}f_\gamma(z_1,z_2), \end{aligned} \tag{A11}$$

with $f_\gamma(z_1,z_2) = (z_1 + \gamma^2 z_2)\frac{1+\gamma^2+\frac{1}{2}\sqrt{(1+\gamma^2)^2-(z_1+\gamma^2z_2)^2}}{\sqrt{1+\gamma^2+\sqrt{(1+\gamma^2)^2-(z_1+\gamma^2z_2)^2}}}$.

APPENDIX B: FIXED POINT AND THE STABILITY ANALYSIS

The fixed point of the system is given by the stationary solution of Eq. (A11), which is obtained by setting all the derivatives as zero, yielding

$$\begin{aligned} &\sqrt{1-z_1^2}\sin\phi_1^s=0,\quad \sqrt{1-z_2^2}\sin\phi_2^s=0,\\ &\Lambda_{\rm MF}\big(z_1^s-\gamma z_2^s\big)+\frac{z_1^s}{\sqrt{1-\left(z_1^s\right)^2}}\cos\phi_1^s+\Lambda_{\rm LHY}f_\gamma\big(z_1^s,z_2^s\big)=0,\\ &\Lambda_{\rm MF}\gamma(\gamma z_2^s-z_1^s)+\frac{z_2^s}{\sqrt{1-\left(z_2^s\right)^2}}\cos\phi_2^s+\Lambda_{\rm LHY}\gamma^2f_\gamma\big(z_1^s,z_2^s\big)=0. \end{aligned}\tag{B1}$$

Solving the first two equations, one has $\phi_i^s=0$ or π $(i=1,2)$, while z_i^s is obtained from the last two equations in above, which depending on ϕ_i^s. To study the stability of the resultant fixed point, we consider small fluctuations $(\delta z_i,\delta\phi_i)$ around the stationary point (z_i^s,ϕ_i^s), i.e. $z_i=z_i^s+\delta z_i$ and $\phi_i=\phi_i^s+\delta\phi_i$, and then linearize Eqs. (A11) to obtain:

$$\begin{aligned} &\delta\dot z_i=-\sqrt{1-(z_i^s)^2}\cos\phi_i^s\delta\phi_i,\\ &\delta\dot\phi_i=\Lambda_{\rm MF}(-\gamma)^{(i-1)}(\delta z_1-\gamma\delta z_2)+\left[1-\left(z_i^s\right)^2\right]^{-\frac{3}{2}}\cos\phi_i^s\delta z_i+\Lambda_{\rm LHY}\gamma^{2(i-1)}f_\gamma'\big(\delta z_1+\gamma^2\delta z_2\big), \end{aligned}\tag{B2}$$

where we have taken use of Eq. (B1) and

$$f_\gamma'=\frac{\partial f}{\partial z}|_{z=z_1^s+\gamma^2z_2^s}=\frac{\frac{3}{2}(1+\gamma^2)^2+\frac{3}{2}(1+\gamma^2)\sqrt{(1+\gamma^2)^2-\left(z_1^s+\gamma^2z_2^s\right)^2}-\frac{3}{4}\left(z_1^s+\gamma^2z_2^s\right)^2}{(1+\gamma^2+\sqrt{(1+\gamma^2)^2-\left(z_1^s+\gamma^2z_2^s\right)^2})^{\frac{3}{2}}}.\tag{B3}$$

From Eq. (B2), we have

$$\begin{pmatrix}\delta\ddot z_1\\ \delta\ddot z_2\end{pmatrix}=\mathcal{M}\begin{pmatrix}\delta z_1\\ \delta z_2\end{pmatrix},\tag{B4}$$

where $\mathcal{M}$ is a 2×2 drift matrix with the elements

$$\begin{aligned} &\mathcal{M}_{11}=-\Lambda_{\rm MF}\sqrt{1-(z_1^s)^2}\cos\phi_1^s-\frac{1}{1-(z_1^s)^2}-\Lambda_{\rm LHY}\sqrt{1-(z_1^s)^2}\cos\phi_1^sf_\gamma',\\ &\mathcal{M}_{12}=\gamma\Lambda_{\rm MF}\sqrt{1-(z_1^s)^2}\cos\phi_1^s-\gamma^2\Lambda_{\rm LHY}\sqrt{1-(z_1^s)^2}\cos\phi_1^sf_\gamma',\\ &\mathcal{M}_{21}=\gamma\Lambda_{\rm MF}\sqrt{1-(z_2^s)^2}\cos\phi_2^s-\gamma^2\Lambda_{\rm LHY}\sqrt{1-(z_2^s)^2}\cos\phi_2^sf_\gamma',\\ &\mathcal{M}_{22}=-\gamma^2\Lambda_{\rm MF}\sqrt{1-(z_2^s)^2}\cos\phi_2^s-\frac{1}{1-(z_2^s)^2}-\gamma^4\Lambda_{\rm LHY}\sqrt{1-(z_2^s)^2}\cos\phi_2^sf_\gamma'. \end{aligned}\tag{B5}$$

Diagonalizing $\mathcal{M}$, we arrive at two eigenfrequencies

$$\omega_\pm^2=\tfrac{1}{2}(-\mathcal{M}_{11}-\mathcal{M}_{22}\pm\sqrt{(\mathcal{M}_{11}-\mathcal{M}_{22})^2+4\mathcal{M}_{12}\mathcal{M}_{21}}).\tag{B6}$$

A stable fixed point requires $\omega_\pm^2\geqslant0$, and the critical value is given by the lower branch with $\omega_-=0$, which gives $\mathcal{M}_{11}\mathcal{M}_{22}=\mathcal{M}_{12}\mathcal{M}_{21}$.

Before proceeding, we notice that there always exists a zero solution $z_1^s=z_2^s=0$ for all cases, while the nonzero solution always appears in a pair with the form of $\pm(z_1^s,z_2^s)\neq0$ due to the Z_2 symmetry. In the following, we mainly discuss the nonzero (stationary) solutions and their stabilities in different cases with $(\phi_1^s,\phi_2^s)=(\pi,\pi)$, $(0,\pi)$, $(\pi,0)$, and (0,0). We will see that the LHY correction can induce a series of unique nontrivial fixed points, which play essential roles in the collective dynamics.

Case I: $(\phi_1^s,\phi_2^s)=(0,0)$. In this case, only the zero solution $z_1^s=z_2^s=0$ exists, corresponding to the ground state of the system.

Case II: $(\phi_1^s,\phi_2^s)=(\pi,\pi)$. In this case, a pair of nonzero solutions $\pm(z_1^s,z_2^s)$ $(z_1^s\geqslant-z_2^s>0)$ appear in the mean field when $\Lambda_{\rm MF}>\Lambda_{\rm MF}^c=\frac{1}{1+\gamma^2}$ for $\Lambda_{\rm LHY}=0$, which are dynamically stable and become antisymmetric $(z_1^s=-z_2^s)$ for $\gamma=1$ with $\Lambda_{\rm MF}^c=\frac{1}{2}$. While beyond mean field with $\Lambda_{\rm LHY}>0$, new

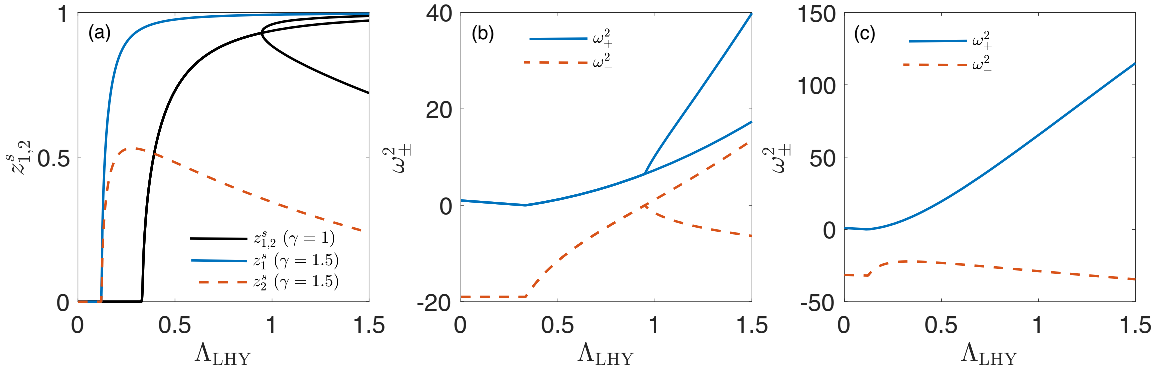

FIG. 6. Nonzero fixed points $z^s_{1,2}$ (a) and the corresponding eigenfrequencies $\omega^2_\pm$ (b), (c) of small fluctuations in the π/π case. Here, $\gamma=1$ for (b), and $\gamma=1.5$ for (c). $\Lambda_{\rm MF}=10$.

asymmetric solutions $\pm(z^s_1,z^s_2)$ $(z^s_1\geqslant z^s_2>0)$ develop when $\Lambda_{\rm LHY}>\Lambda^c_{\rm LHY}$ with

$$\Lambda^c_{\rm LHY}=\frac{2\sqrt{2}}{3\sqrt{1+\gamma^2}}\frac{\Lambda_{\rm MF}+\Lambda_{\rm MF}\gamma^2-1}{\Lambda_{\rm MF}\gamma^2+2\Lambda_{\rm MF}\gamma^3+\Lambda_{\rm MF}\gamma^4-\gamma^4-1}. \tag{B7}$$

Specifically for $\gamma=1$, the above asymmetric solutions are symmetric $(z^s_1=z^s_2)$ with $\Lambda^c_{\rm LHY}=\frac{1}{3}$, which is independent on the mean field parameter $\Lambda_{\rm MF}$. More interestingly for $\gamma=1$, besides the Z_2 symmetry, there is another symmetry that Eq. (B1) is invariant by exchanging $z^s_1\leftrightarrow z^s_2$. This gives rise to another two pairs of asymmetric solutions $\pm(z^s_1,z^s_2)$, $\pm(z^s_2,z^s_1)$ $(z^s_1>z^s_2>0)$ when $\Lambda_{\rm LHY}>\Lambda^*_{\rm LHY}$ with

$$\Lambda^*_{\rm LHY}=\frac{(2\Lambda_{\rm MF})^{\frac{1}{3}}\sqrt{1+(2\Lambda_{\rm MF})^{-\frac{1}{3}}}}{\sqrt{2}[2+(2\Lambda_{\rm MF})^{-\frac{1}{3}}]}. \tag{B8}$$

As shown in Fig. 6, these asymmetric solutions are dynamically unstable, while the symmetric ones become stable when $\Lambda_{\rm LHY}\geqslant\Lambda^*_{\rm LHY}$, where $\omega_-=0$ for $\Lambda_{\rm LHY}=\Lambda^*_{\rm LHY}$.

Case III: $(\phi^s_1,\phi^s_2)=(\pi,0)$ *or* $(0,\pi)$. In the mean field with $\Lambda_{\rm LHY}=0$, there is only zero solution for both cases. While in the presence of LHY term, nonzero solutions can exist with the (asymmetric) fixed points and corresponding critical LHY parameters given by

$$(\pi,0):\ \pm(z^s_1,z^s_2)\,(z^s_1>z^s_2>0),$$

$$\Lambda^c_{\rm LHY}=\frac{2\sqrt{2}}{3\sqrt{1+\gamma^2}}\frac{-\Lambda_{\rm MF}+\Lambda_{\rm MF}\gamma^2+1}{\Lambda_{\rm MF}\gamma^2+2\Lambda_{\rm MF}\gamma^3+\Lambda_{\rm MF}\gamma^4-\gamma^4+1}, \tag{B9}$$

and

$$(0,\pi):\ \pm(z^s_1,z^s_2)\,(z^s_2>z^s_1>0),$$

$$\Lambda^c_{\rm LHY}=\frac{2\sqrt{2}}{3\sqrt{1+\gamma^2}}\frac{\Lambda_{\rm MF}-\Lambda_{\rm MF}\gamma^2+1}{\Lambda_{\rm MF}\gamma^2+2\Lambda_{\rm MF}\gamma^3+\Lambda_{\rm MF}\gamma^4+\gamma^4-1}. \tag{B10}$$

For $\gamma=1$, above solutions for both cases relate to each other under $z^s_1\leftrightarrow z^s_2$ with the same $\Lambda^c_{\rm LHY}=\frac{1}{6\Lambda_{\rm MF}}$. Notice that from Eq. (B10) of the $(0,\pi)$ case, we have $\Lambda^c_{\rm LHY}\leqslant 0$ when $\gamma\geqslant\sqrt{1+\frac{1}{\Lambda_{\rm MF}}}$, meaning that the nonzero solutions induced by the LHY correction in the $(0,\pi)$ case can survive in the mean field if the interactions are sufficiently asymmetric. As shown in Fig. 7, except for $\Lambda^{\star,1}_{\rm LHY}<\Lambda_{\rm LHY}<\Lambda^{\star,2}_{\rm LHY}$ where the eigenfrequencies $\omega_\pm$ have imaginary parts [i.e., $(\mathcal{M}_{11}-\mathcal{M}_{22})^2+4\mathcal{M}_{12}\mathcal{M}_{21}<0$] and thus are unstable [referred to the dashed lines in Figs. 7(d) and 7(e)], the asymmetric solutions in these two cases are stable against small perturbations, indicating the "π-phase" self-trapping around these fixed points.

APPENDIX C: LHY EFFECT FOR $\delta g>0$

In this section, we consider a general case with $\delta g>0$, such that both branches in the LHY correction (A2) would contribute to the collective dynamics. Similar to the first section, after a tedious but straightforward derivation, we can obtain the dimensionless dynamical equations for the relative number difference z_i and phase difference ϕ_i, which are

$$\dot z_i=-\sqrt{1-z_i^2}\sin\phi_i,$$

$$\dot\phi_i=\Lambda_{\rm MF}\gamma^{2(i-1)}z_i+\Lambda_{\rm MF}\beta z_{j\neq i}+\frac{z_i}{\sqrt{1-z_i^2}}\cos\phi_i+\frac{1}{16}\Lambda_{\rm LHY}\gamma^{2(i-1)}\left(\mu^{(1)}_++\mu^{(1)}_--\mu^{(2)}_+-\mu^{(2)}_-\right). \tag{C1}$$

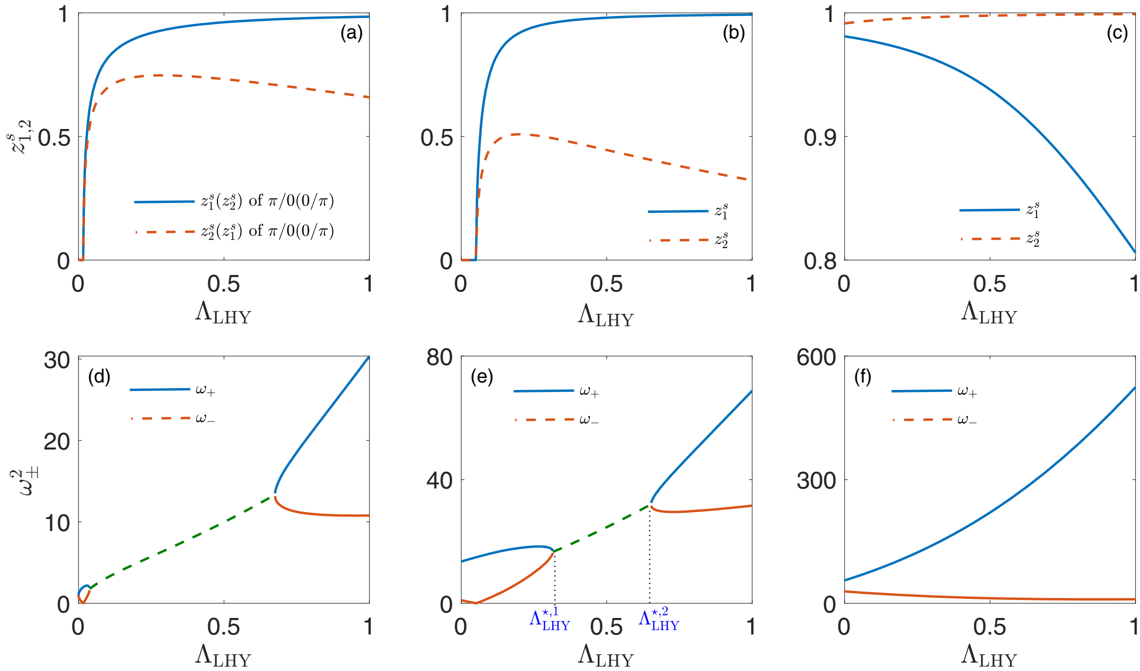

FIG. 7. Nonzero fixed points $z^s_{1,2}$ (a)–(c) and the corresponding eigenfrequencies $\omega^2_\pm$ (d)–(f) of small fluctuations in the $\pi/0$ (a), (b), (d), (e) and $0/\pi$ (a), (c), (d), (f) cases. The green-dashed lines in (d) and (e) denote the real parts of $\omega_\pm$ where the imaginary parts are not zero for $\Lambda^{\star,1}_{\rm LHY} < \Lambda_{\rm LHY} < \Lambda^{\star,2}_{\rm LHY}$ and thus unstable. Here, $\gamma = 1$ for (a) and (d), and $\gamma = 1.5$ for others. $\Lambda_{\rm MF} = 10$.

Here

$$\begin{aligned}
\mu_+^{(1)} &= \left(1 + \frac{1 + z_1 - \gamma^2(1+z_2) + 2\beta^2(1+z_2)}{\kappa_+}\right)\left(1 + z_1 + \gamma^2 + \gamma^2 z_2 + \kappa_+\right)^{\frac{3}{2}},\\
\mu_-^{(1)} &= \left(1 - \frac{1 + z_1 - \gamma^2(1+z_2) + 2\beta^2(1+z_2)}{\kappa_+}\right)\left(1 + z_1 + \gamma^2 + \gamma^2 z_2 - \kappa_+\right)^{\frac{3}{2}},\\
\mu_+^{(2)} &= \left(1 + \frac{-(1 - z_1) + \gamma^2(1-z_2) + 2\frac{\beta^2}{\gamma^2}(1-z_1)}{\kappa_-}\right)\left(1 - z_1 + \gamma^2 - \gamma^2 z_2 + \kappa_-\right)^{\frac{3}{2}},\\
\mu_-^{(2)} &= \left(1 - \frac{-(1 - z_1) + \gamma^2(1-z_2) + 2\frac{\beta^2}{\gamma^2}(1-z_1)}{\kappa_-}\right)\left(1 - z_1 + \gamma^2 - \gamma^2 z_2 - \kappa_-\right)^{\frac{3}{2}},
\end{aligned} \tag{C2}$$

with

$$\kappa_\pm = \sqrt{[1 \pm z_1 - \gamma^2(1 \pm z_2)]^2 + 4\beta^2(1 \pm z_1)(1 \pm z_2)}, \tag{C3}$$

and $\beta \equiv \frac{g_{12}}{g_{11}}$ (< 0). We further introduce a dimensionless $\delta_g \equiv \frac{\delta g}{g_{11}} = \beta + \gamma$. Then for $\beta = -\gamma$, we have $\delta g = 0$ and Eq. (A11) is recovered. For a general $\delta g > 0$, one can solve Eq. (C1) to find the dynamical evolutions as well as the fixed points of the system. In Fig. 8, we give the evolutions of z_i and ϕ_i for $\delta_g = 0.05$ under the same initial conditions used in the main text. We can see that similar dynamical behaviors can be identified in different cases, suggesting the main results discussed in the main text would be not changed essentially for $\delta_g > 0$. Moreover, the threshold LHY parameter to trigger the MQST is found to be even lower than the case of $\delta_g = 0$, which is reflected on the decreasing of the critical LHY parameter $\Lambda^c_{\rm LHY}$ for nontrivial fixed points with δg, as shown in the main text.

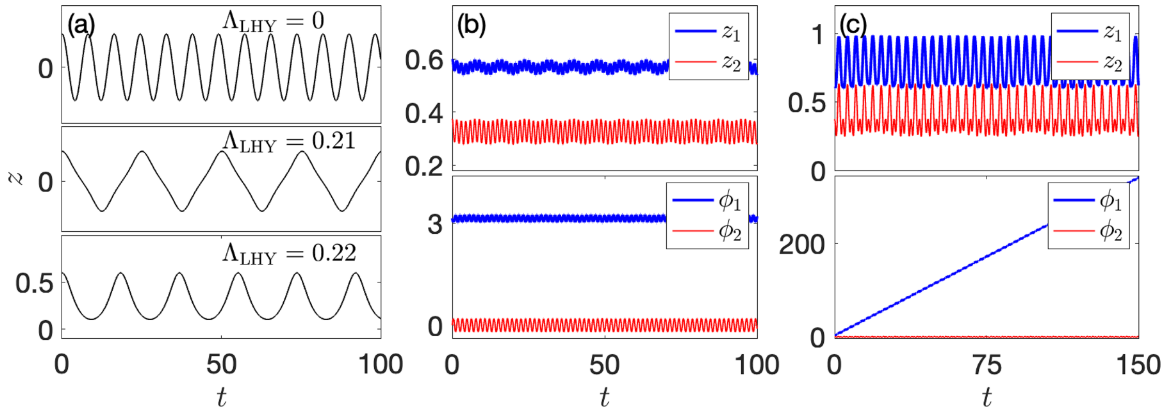

FIG. 8. (a) Time evolution of $z(t)$ for $\Lambda_{\rm LHY} = 0$ (top), 0.21 (middle), and 0.22 (bottom); time evolutions of $z_i(t)$ and $\phi_i(t)$ at $\gamma = 1.6$ for (b) $\Lambda_{\rm LHY} = 0.02$ and (c) $\Lambda_{\rm LHY} = 0.16$. The initial conditions are $[z(0), \phi(0)] = [0.6, \pi]$ for (a) and $[z_1(0), \phi_1(0), z_2(0), \phi_2(0)] = [0.6, \pi, 0.4, 0]$ for (c). Here, $\delta_g = 0.05$ and $\Lambda_{\rm MF} = 10$.

[1] T. D. Lee, K. Huang, and C. N. Yang, Eigenvalues and eigenfunctions of a Bose system of hard spheres and its low-temperature properties, Phys. Rev. **106**, 1135 (1957).

[2] D. M. Larsen, Binary mixtures of dilute Bose gases with repulsive interactions at low temperature, Ann. Phys. **24**, 89 (1963).

[3] D. S. Petrov, Quantum mechanical stabilization of a collapsing Bose-Bose mixture, Phys. Rev. Lett. **115**, 155302 (2015).

[4] D. S. Petrov and G. E. Astrakharchik, Ultradilute low-dimensional liquids, Phys. Rev. Lett. **117**, 100401 (2016).

[5] P. Cheiney, C. R. Cabrera, J. Sanz, B. Naylor, L. Tanzi, and L. Tarruell, Bright soliton to quantum droplet transition in a mixture of Bose-Einstein condensates, Phys. Rev. Lett. **120**, 135301 (2018).

[6] C. R. Cabrera, L. Tanzi, J. Sanz, B. Naylor, P. Thomas, P. Cheiney, and L. Tarruell, Quantum liquid droplets in a mixture of Bose-Einstein condensates, Science **359**, 301 (2018).

[7] G. Semeghini, G. Ferioli, L. Masi, C. Mazzinghi, L. Wolswijk, F. Minardi, M. Modugno, G. Modugno, M. Inguscio, and M. Fattori, Self-bound quantum droplets in atomic mixtures in free space, Phys. Rev. Lett. **120**, 235301 (2018).

[8] C. D'Errico, A. Burchianti, M. Prevedelli, L. Salasnich, F. Ancilotto, M. Modugno, F. Minardi, and C. Fort, Observation of quantum droplets in a heteronuclear bosonic mixture, Phys. Rev. Res. **1**, 033155 (2019).

[9] M. Schmitt, M. Wenzel, F. Böttcher, I. Ferrier-Barbut, and T. Pfau, Self-bound droplets of a dilute magnetic quantum liquid, Nature (London) **539**, 259 (2016).

[10] I. Ferrier-Barbut, H. Kadau, M. Schmitt, M. Wenzel, and T. Pfau, Observation of quantum droplets in a strongly dipolar Bose gas, Phys. Rev. Lett. **116**, 215301 (2016).

[11] C. Mishra, L. Santos, and R. Nath, Self-bound doubly dipolar Bose-Einstein condensates, Phys. Rev. Lett. **124**, 073402 (2020).

[12] J. C. Smith, D. Baillie, and P. B. Blakie, Quantum droplet states of a binary magnetic gas, Phys. Rev. Lett. **126**, 025302 (2021).

[13] N. B. Jørgensen, G. M. Bruun, and J. J. Arlt, Dilute fluid governed by quantum fluctuations, Phys. Rev. Lett. **121**, 173403 (2018).

[14] T. G. Skov, M. G. Skou, N. B. Jø rgensen, and J. J. Arlt, Observation of a Lee-Huang-Yang fluid, Phys. Rev. Lett. **126**, 230404 (2021).

[15] Y. V. Kartashov, B. A. Malomed, L. Tarruell, and L. Torner, Three-dimensional droplets of swirling superfluids, Phys. Rev. A **98**, 013612 (2018).

[16] G. Ferioli, G. Semeghini, L. Masi, G. Giusti, G. Modugno, M. Inguscio, A. Gallemí, A. Recati, and M. Fattori, Collisions of self-bound quantum droplets, Phys. Rev. Lett. **122**, 090401 (2019).

[17] X. Zhang, X. Xu, Y. Zheng, Z. Chen, B. Liu, C. Huang, B. A. Malomed, and Y. Li, Semidiscrete quantum droplets and vortices, Phys. Rev. Lett. **123**, 133901 (2019).

[18] L. He, P. Gao, and Z.-Q. Yu, Normal-superfluid phase separation in spin-half bosons at finite temperature, Phys. Rev. Lett. **125**, 055301 (2020).

[19] H. Hu and X.-J. Liu, Consistent theory of self-bound quantum droplets with bosonic pairing, Phys. Rev. Lett. **125**, 195302 (2020).

[20] R. N. Bisset, L. A. Peña Ardila, and L. Santos, Quantum droplets of dipolar mixtures, Phys. Rev. Lett. **126**, 025301 (2021).

[21] Y. Ma, C. Peng, and X. Cui, Borromean droplet in three-component ultracold Bose gases, Phys. Rev. Lett. **127**, 043002 (2021).

[22] L. Lavoine, A. Hammond, A. Recati, D. S. Petrov, and T. Bourdel, Beyond-mean-field effects in rabi-coupled two-component Bose-Einstein condensate, Phys. Rev. Lett. **127**, 203402 (2021).

[23] L. Dong and Y. V. Kartashov, Rotating multidimensional quantum droplets, Phys. Rev. Lett. **126**, 244101 (2021).

[24] Z.-H. Luo, W. Pang, B. Liu, Y.-Y. Li, and B. A. Malomed, A new form of liquid matter: Quantum droplets, Front. Phys. **16**, 32201 (2021).

[25] F. Böttcher, J. Schmidt, J. Hertkorn, K. S. H. Ng, S. D. Graham, M. Guo, T. Langen, and T. Pfau, New states of matter with fine-tuned interactions: quantum droplets and dipolar supersolids, Rep. Prog. Phys. **84**, 012403 (2021).

[26] R. Gati and M. K. Oberthaler, A bosonic Josephson junction, J. Phys. B: At. Mol. Opt. Phys. **40**, R61 (2007).

[27] M. Albiez, R. Gati, J. Fölling, S. Hunsmann, M. Cristiani, and M. K. Oberthaler, Direct observation of tunneling and nonlinear self-trapping in a single bosonic Josephson junction, Phys. Rev. Lett. **95**, 010402 (2005).

[28] S. Levy, E. Lahoud, I. Shomroni, and J. Steinhauer, The a.c. and d.c. Josephson effects in a Bose-Einstein condensate, Nature (London) **449**, 579 (2007).

[29] A.-C. Ji, Q. Sun, X. C. Xie, and W. M. Liu, Josephson effect for photons in two weakly linked microcavities, Phys. Rev. Lett. **102**, 023602 (2009).

[30] T. Zibold, E. Nicklas, C. Gross, and M. K. Oberthaler, Classical bifurcation at the transition from Rabi to Josephson dynamics, Phys. Rev. Lett. **105**, 204101 (2010).

[31] M. Abbarchi, A. Amo, V. G. Sala, D. D. Solnyshkov, H. Flayac, L. Ferrier, I. Sagnes, E. Galopin, A. Lemaître, G. Malpuech, and J. Bloch, Macroscopic quantum self-trapping and Josephson oscillations of exciton polaritons, Nat. Phys. **9**, 275 (2013).

[32] G. Spagnolli, G. Semeghini, L. Masi, G. Ferioli, A. Trenkwalder, S. Coop, M. Landini, L. Pezzè, G. Modugno, M. Inguscio, A. Smerzi, and M. Fattori, Crossing over from attractive to repulsive interactions in a tunneling bosonic Josephson junction, Phys. Rev. Lett. **118**, 230403 (2017).

[33] A. Smerzi, S. Fantoni, S. Giovanazzi, and S. R. Shenoy, Quantum coherent atomic tunneling between two trapped Bose-Einstein condensates, Phys. Rev. Lett. **79**, 4950 (1997).

[34] S. Raghavan, A. Smerzi, S. Fantoni, and S. R. Shenoy, Coherent oscillations between two weakly coupled Bose-Einstein condensates: Josephson effects, π oscillations, and macroscopic quantum self-trapping, Phys. Rev. A **59**, 620 (1999).

[35] S. Ashhab and C. Lobo, External Josephson effect in Bose-Einstein condensates with a spin degree of freedom, Phys. Rev. A **66**, 013609 (2002).

[36] H. T. Ng, C. K. Law, and P. T. Leung, Quantum-correlated double-well tunneling of two-component Bose-Einstein condensates, Phys. Rev. A **68**, 013604 (2003).

[37] Ö. E. Müstecaplıoğlu, W. Zhang, and L. You, Quantum dynamics of a spin-1 condensate in a double-well potential, Phys. Rev. A **75**, 023605 (2007).

[38] B. Juliá-Díaz, M. Guilleumas, M. Lewenstein, A. Polls, and A. Sanpera, Josephson oscillations in binary mixtures of $F = 1$ spinor Bose-Einstein condensates, Phys. Rev. A **80**, 023616 (2009).

[39] H. Qiu, J. Tian, and L.-B. Fu, Collective dynamics of two-species Bose-Einstein-condensate mixtures in a double-well potential, Phys. Rev. A **81**, 043613 (2010).

[40] M. Chuchem, K. Smith-Mannschott, M. Hiller, T. Kottos, A. Vardi, and D. Cohen, Quantum dynamics in the bosonic Josephson junction, Phys. Rev. A **82**, 053617 (2010).

[41] See the Appendix for the details of the derivations of the model, the fixed points and the stability analysis, and the case where both branches of the LHY corrections would contribute.

[42] The nonzero fixed points in the $\pi/0$ and $0/\pi$ cases are mostly stable, except an intermediate regime of the LHY parameter, see Table II and the Appendix for more details.

[43] P. Coullet and N. Vandenberghe, Chaotic self-trapping of a weakly irreversible double Bose condensate, Phys. Rev. E **64**, 025202(R) (2001).

[44] E. Boukobza, M. G. Moore, D. Cohen, and A. Vardi, Nonlinear phase dynamics in a driven bosonic Josephson junction, Phys. Rev. Lett. **104**, 240402 (2010).

[45] W.-C. Syu, D.-S. Lee, and C.-Y. Lin, Regular and chaotic behavior of collective atomic motion in two-component Bose-Einstein condensates, Phys. Rev. A **101**, 063622 (2020).

[46] C. Chin, R. Grimm, P. Julienne, and E. Tiesinga, Feshbach resonances in ultracold gases, Rev. Mod. Phys. **82**, 1225 (2010).

[47] S. Giorgini, J. Boronat, and J. Casulleras, Ground state of a homogeneous Bose gas: A diffusion Monte Carlo calculation, Phys. Rev. A **60**, 5129 (1999).

[48] A. Hampton and D. H. Zanette, Measure synchronization in coupled hamitonian systems, Phys. Rev. Lett. **83**, 2179 (1999).

[49] J. Tian, H. Qiu, G. Wang, Y. Chen, and L.-B. Fu, Measure Synchronization in a two-species bosonic Josephson junction, Phys. Rev. E **88**, 032906 (2013).